Research Square

Preprints are preliminary reports that have not undergone peer review.
They should not be considered conclusive, used to inform clinical practice,
or referenced by the media as validated information.

An oleaginous Solicoccozyma sp. from the Yungas cloud forest couples phenol removal with lipid production

Facundo Gabriel Dominguez
PROIMI, CONICET (Planta Piloto de Procesos Industriales Microbiológicos)
Natalia Daniela Alancay Rojas
PROIMI, CONICET (Planta Piloto de Procesos Industriales Microbiológicos)
Mariana Soledad Pacheco
PROIMI, CONICET (Planta Piloto de Procesos Industriales Microbiológicos)
Carlos Gabriel Nieto-Peñalver
PROIMI, CONICET (Planta Piloto de Procesos Industriales Microbiológicos)
Hipolito Fernando Pajot
hipolitopajot@conicet.gov.ar
PROIMI, CONICET (Planta Piloto de Procesos Industriales Microbiológicos)

Research Article

Keywords: Oleaginous yeast, phenol removal, microbial lipids, Solicoccozyma, bioremediation, Las Yungas cloud forest

Posted Date: November 23rd, 2026

DOI: https://doi.org/10.21203/rs.3.rs-11716264/v1

License: This work is licensed under a Creative Commons Attribution 4.0 International License.
Read Full License

Additional Declarations: No competing interests reported.

Abstract

The ability to sustain lipid production during exposure to toxic aromatic compounds represents an important challenge in the biotechnological exploitation of oleaginous yeasts, yet the physiological responses of less-studied yeast taxa to phenol exposure remain poorly characterized. In this study, yeasts isolated from Las Yungas cloud forest in northwestern Argentina were screened for aromatic compound tolerance and lipid accumulation, leading to the selection of *Solicoccozyma* sp. F6BS1. During the initial screening, the isolate accumulated 55.8% lipids (w/w), reaching 7.45 g L^{-1} in phenol-free medium. Subsequent characterization in glucose-containing medium supplemented with 0.5 g L^{-1} phenol revealed approximately 82% phenol removal within 120 h. Despite an initial delay in biomass accumulation and glucose consumption, lipid production reached 7.83 g L^{-1} after 144 h, compared with 7.34 g L^{-1} in the phenol-free control. The fatty acid profile was dominated by C16:0 and C18:1, with no major changes under phenol exposure. Catechol 1,2-dioxygenase activity was detected, reaching 0.304 ± 0.039 U mg^{-1} protein, whereas catechol 2,3-dioxygenase activity was not detected. These findings suggest the possible involvement of an ortho-cleavage pathway in phenol transformation and expand current knowledge of the physiological versatility of *Solicoccozyma*, highlighting its potential for biotechnological processes combining aromatic pollutant removal with microbial lipid production.

Highlights

• An oleaginous *Solicoccozyma* sp. was isolated from the Yungas cloud forest.

• The selected isolate accumulated up to 55.8% lipids in phenol-free medium.

• Phenol removal reached 82% while substantial lipid production was maintained.

• Catechol 1,2-dioxygenase activity suggests a possible ortho-cleavage pathway.

• The findings expand the biotechnological potential of *Solicoccozyma* yeasts.

Introduction

Phenol and its derivatives are common aromatic pollutants found in the waste streams of various industrial processes, including oil refining, organic compound manufacturing, and olive processing (Ahmaruzzaman et al., 2024). These compounds are highly toxic to aquatic life and have been linked to severe health problems in humans and animals, including mutagenic, carcinogenic, and teratogenic effects (Duan et al., 2018; Panigrahy et al., 2020). Natural phenol degradation proceeds at very low rates, often taking decades. Consequently, intensified industrial activities have led to environmental accumulation, making phenols a significant and growing threat to ecosystem health and human well-being (Wu et al., 2022). A promising solution to this problem lies in the utilization of specialized microorganisms capable of degrading aromatic compounds (Panigrahy et al., 2020). Among these, oleaginous yeasts offer a unique biotechnological advantage: their metabolic flexibility allows them to

channel aromatic degradation intermediates, such as acetyl-CoA and pyruvate, directly into fatty acid biosynthesis, effectively coupling pollutant removal with lipid accumulation (Yaguchi et al., 2020).

Microbial lipids, also known as single-cell oils (SCOs), have emerged as sustainable alternatives to vegetable oil-based biodiesel, offering the potential to reduce reliance on agricultural land intended for food production and biodiversity conservation (Ramalingam et al., 2023; Sánchez-Solís et al., 2024). Furthermore, the production of high-value lipids, including omega-3, -6, and – 9 fatty acids, nervonic acid, and other polyunsaturated fatty acids (PUFAs), has garnered significant interest due to their economic viability in industrial applications (Poontawee et al., 2023; Szczepańska et al., 2022). However, lipid profiles in SCOs are highly strain-dependent (Sapsirisuk et al., 2022), and current research remains heavily biased toward a few model genera, such as *Cutaneotrichosporon, Rhodotorula, Lipomyces*, and *Yarrowia* (Abeln and Chuck, 2021). This limited exploration of microbial diversity constrains the discovery of strains with optimal lipid profiles. Identifying yeasts capable of both degrading aromatic pollutants and accumulating lipids with distinctive compositions would enable integrated bioprocesses coupling bioremediation with value-added product generation.

While phenol-degrading microorganisms have been isolated from contaminated sites (Harzallah et al., 2023; Sun et al., 2023), pristine environments harbor microorganisms with metabolic capabilities for aromatic compound assimilation that remain largely unexplored. Cloud forests are biodiversity hotspots (Velez et al., 2021) where the decomposition of lignocellulosic material generates phenolic compounds and other aromatic molecules (Liu et al., 2024; Wang et al., 2020), creating selective pressure that favors microorganisms capable of metabolizing these compounds (Torres et al., 2014; Wu et al., 2023). In this context, the montane cloud forests of Las Yungas in northwestern Argentina represent a promising, underexplored reservoir for novel oleaginous yeasts. This ecosystem is characterized by minimal anthropogenic disturbance and the presence of *Podocarpus parlatorei*, one of the few conifer species endemic to South America (Entrocassi et al., 2020; Peralta et al., 2021). The geographic isolation of this endemic tree, combined with the distinct chemical signature of its rhizosphere, creates a unique ecological niche that may harbor specialized yeast lineages with metabolic versatility for aromatic assimilation.

Thus, the present study reports the isolation and characterization of an oleaginous yeast from Las Yungas capable of simultaneously removing phenol and sustaining substantial lipid accumulation, establishing a foundation for integrated bioprocesses that couple aromatic pollutant removal with microbial lipid production.

Materials and Methods

Isolation of phenol-tolerant yeast from Podocarpus parlatorei trees and associated soil

Soil and bark samples of *Podocarpus parlatorei* were collected from the Alto de Medina hills (26° 26' 0.56" S, 65° 03' 26.5" W) Tucumán, NW Argentina. Samples were obtained from eight *Podocarpus parlatorei* trees with a diameter at breast height greater than 50 cm, spaced 10 meters apart. Bark

samples were collected after removing the superficial layer, while the adjacent soil was sampled by removing the top 10 cm of leaf litter and mulch. The collected samples were then transported in sterile Falcon tubes to the laboratory for further processing.

Enrichment was conducted by adding 1 g of the sample to a 250 mL Erlenmeyer flask containing 100 mL of LBM medium (0.001 g L^{-1} glucose, 0.01 g L^{-1} soybean peptones, and 0.001 g L^{-1} yeast extract) supplemented with chloramphenicol (100 µg mL^{-1}), tetracycline (15 µg mL^{-1}) and 0.5 g L^{-1} phenol, following the method described by Pointing, (1999). Flasks were incubated at 25°C with agitation at 250 rpm for 24 hours. A 1 mL aliquot of the enriched culture was spread onto Petri plates containing solidified LBM medium (12 g L^{-1} agar) supplemented with 0.5 g L^{-1} phenol. Four colonies from each plate, displaying distinct macroscopic traits (e.g., color and colony texture), were selected. These colonies were further purified using exhaustion streaking on Petri plates with LBM medium at pH 5.5 to inhibit bacterial growth, while favoring yeast development. Plates were incubated at 25°C until colony development, as previously described. Pure colonies were classified based on macroscopic features. Axenic cultures were preserved in vials containing 40% glycerol and stored at -80°C for future use.

Phenotypic characterization of yeast isolates

Isolates were classified as Ascomycetes and Basidiomycetes using standard biochemical tests for urease activity and Alkali-ethanol-DBB (Summerbell, 1985). A positive urease result was indicated by a violet color change in the medium, while a purple color change in biomass was considered positive for the DBB test. Isolates that were positive for both Alkali-ethanol-DBB and urease were classified as Basidiomycetes, following the methodology outlined by Kurtzman et al. (2011). *Wickerhamomyces anomalus* M10 (Ascomycetes) and *Apiotrichum domesticum* JCM9580 (Basidiomycetes) were used as internal controls.

Tolerance to aromatic compounds

Isolates were incubated on Petri plates with LBM medium supplemented with phenol (1 g L^{-1}), naphthol (1 g L^{-1}), and anthracene (0.75 g L^{-1}). Growth controls were conducted by inoculating plates with LBM medium, both with and without glucose (1 g L^{-1}). Isolates were classified as tolerant if they showed growth in the supplemented media during the first 72 hours of cultivation. Isolates exhibiting enhanced growth in phenol-supplemented medium compared with the phenol-free control were identified based on biomass production after five days of cultivation.

Characterization of oleaginous isolates

Isolates showing abundant growth in the three tested media after 120 h were selected for lipid production assays in liquid GMY medium, recommended for lipid production(Buzzini, 2001). Fifty-milliliter flasks containing GMY medium (C/N 50) (41.25 g L^{-1} glucose, 3 g L^{-1} yeast extract, 8 g L^{-1}

KH_2PO_4, and 0.5 g L^{-1} $MgSO_4$) were inoculated with 10% (v/v) seed culture (OD_{550} 0.8) to get a final volume of 20 mL. Cultures were cultivated at 25° C and 250 rpm in an orbital shaker. After 120 hours of cultivation, a 4 mL sample was collected to evaluate biomass (g L^{-1}), lipid accumulation (g L^{-1}), and residual reducing sugars (g L^{-1}). Biomass was recovered by centrifugation, washed twice with distilled water, and dried at 105° C to constat weight. Lipids were extracted from the freeze-dried biomass using 1.5 mL of a chloroform:methanol solution (2:1, v/v) with constant shaking at room temperature, following the method of Bligh and Dyer, (1959). The lipid content was determined gravimetrically after drying at 105°C to a constant weight. Residual reducing sugars were quantified spectrophotometrically using the 3,5-dinitrosalicylic acid (DNS) assay (Miller, 1959). Biomass productivity (Q_X) and lipid productivity (Q_L) were determined by dividing their concentrations by the cultivation time and expressed in g L^{-1} h^{-1}. Differences in yield coefficients were analyzed statistically using analysis of variance (ANOVA) followed by Tukey's post-hoc test (Maza et al., 2020). Isolates with a lipid content of ≥ 20% w/w were classified as oleaginous.

Growth and lipid production kinetics of selected isolates

The kinetics of biomass and lipid production, glucose consumption, pH, and phenol were evaluated using 250 mL Erlenmeyer flasks containing 50 mL of GMY medium supplemented with phenol during 144 h. Cultures were inoculated with 10% (v/v) of yeast suspension (OD_{550} 0.8) as previously described and incubated at 25°C with shaking at 250 rpm for 144 h. Samples were periodically collected and centrifuged at 10000 ×g for 10 min. The cell pellet and supernatant were separated and stored at -20°C until further analysis. Biomass, lipids, and residual glucose were analyzed as previously described. Residual phenol in cell-free supernatants (2 mL) was quantified by the 4-aminoantipyrine colorimetric method at 500 nm on a UV–Vis spectrophotometer (Liu et al., 2011).

Molecular identification

DNA extraction was performed using the CTAB method (Doyle, 1991). The quantity and purity of the extracted DNA were assessed spectrophotometrically by measuring absorbance at 260 and 280 nm with a Thermo Scientific™ Multiskan™ GO spectrophotometer. The ITS region and the D1/D2 domain of the 28S ribosomal DNA (LSU) were amplified via PCR using the primers ITS1 (White et al., 1990) and NL4 (O'Donnell, 1993). The sequencing of the PCR products was performed by Macrogen. Consensus sequences were assembled using BioEdit v7.7 (Hall, 1999) and subjected to identity/similarity analysis against sequences in the NCBI database (http://www.ncbi.nlm.nih.gov/) using the nBLAST algorithm (Altschul et al., 1997). Phylogenetic analysis was conducted in PhyloSuite (Zhang et al., 2020). Maximum likelihood phylogenies were reconstructed using IQ-TREE v2.2.0 (Nguyen et al., 2015), with the model automatically selected by the software ('Auto' option), 20,000 ultrafast bootstraps (Minh et al., 2013), and the Shimodaira–Hasegawa-like approximate likelihood-ratio test (Guindon et al., 2010). Reference sequences from curated type material used for phylogenetic reconstruction are listed in Table S1.

Microscopic characterization

For microscopic characterization, culture broth samples grown in the presence and absence of phenol were collected at 120 h (2 mL), centrifuged to concentrate the biomass, and resuspended in 200 µL of distilled water. Intracellular lipid bodies were visualized by fluorescence microscopy after staining with Nile Red (9-diethylamino-5H-benzo[α]phenoxazine-5-one) following the method described by Kimura et al. (2004). Calcofluor White was used as a cell wall stain for live cells at a final concentration of 1 µg mL^{-1} (Hašek, 2006).

Enzymatic assay for phenol degradation pathways

To investigate the possible involvement of catechol ortho- and meta-cleavage pathways in phenol transformation, catechol 1,2-dioxygenase and catechol 2,3-dioxygenase activities were measured in cell-free extracts. Yeast cells grown on phenol (0.5 g L^{-1}) were harvested by centrifugation (8000 ×g, 10 min), washed twice, and resuspended in 50 mM phosphate buffer (pH 7.0). The cell suspension was disrupted by sonication (20 kHz, 15 min) and centrifuged (8000 ×g, 5 min). The resulting supernatant was collected and used as the cell-free extract. The total protein concentration of this extract was determined using the Bradford method with a Bovine Serum Albumin (BSA) calibration curve (Kruger, 2009). Enzyme activities were assayed in 3.0 mL reaction mixtures containing 1.0 mL of cell-free extract and catechol as the substrate. For catechol 1,2-dioxygenase (ortho-cleavage), the mixture contained 0.8 mM catechol, 50 mM Tris–HCl buffer (pH 8.0), and 0.1 mM 2-mercaptoethanol; absorbance was measured at 260 nm, corresponding to the formation of cis,cis-muconic acid. For catechol 2,3-dioxygenase (meta-cleavage), the mixture contained 0.3 mM catechol in 50 mM phosphate buffer (pH 7.0); absorbance was measured at 375 nm, corresponding to the formation of 2-hydroxymuconic semialdehyde (Shetty and Shetty, 2016). Enzyme activities were expressed as µmol of product formed per minute, calculated using molar extinction coefficients of ε_{260} = 16,800 L mol^{-1} cm^{-1} for catechol 1,2-dioxygenase and ε_{375} = 14,700 L mol^{-1} cm^{-1} for catechol 2,3-dioxygenase. Specific activities were expressed as units per milligram of protein (U mg^{-1} protein).

Lipid profile characterization

A total of 20 mg of lipids were weighed into glass test tubes and transesterified using methanolic sulfuric acid to produce fatty acid methyl esters (FAMEs). The FAMEs were analyzed using a Thermo Scientific™ Trace™ 1310 gas chromatography system with a glass capillary silica column. The column temperature was programmed to ramp from 50 °C to 200 °C, with a hold at 200 °C for 25 minutes. Identification of the FAMEs was achieved by comparing their mass spectra with the NIST library. The relative concentration of each FAME was determined by analyzing the peak areas in the chromatograms. Empirical biodiesel properties were estimated using mathematical formulas as described by Maza et al., (2020).

Results

Isolation and aromatic compounds tolerance of isolated yeast

Phenol enrichment (0.5 g L^{-1}) yielded 69 yeast isolates, 18 of which were excluded due to slow growth. The remaining 51 isolates, obtained from two substrates (bark: 23 isolates; soil: 28 isolates), were subjected to biochemical tests (urease and DBB) for differentiation. Specifically, bark samples yielded 8 Ascomycetes and 15 Basidiomycetes, while soil samples yielded 19 Ascomycetes and 9 Basidiomycetes, totaling 27 Ascomycetes and 24 Basidiomycetes. Among bark isolates, Ascomycetes showed tolerance values of 62% for β-naphthol, 100% for anthracene, and 62% for phenol, whereas Basidiomycetes exhibited consistently high tolerance (93%) to all tested compounds (Figure S1). For soil isolates, Ascomycetes displayed tolerance values of 68% for β-naphthol, 84% for anthracene, and 63% for phenol. In contrast, Basidiomycetes reached 100% tolerance for β-naphthol and anthracene, and 89% for phenol. Overall, Basidiomycetes exhibited higher tolerance frequencies than Ascomycetes across both substrates. Based on these results, thirteen isolates (namely, F1AC2, F1AC4, F2AS1, F2AS3, F4AC1, F4AC2, F4AC3, F4AC4, F7BC1, F7BC3, F6BS1, F6AC1, and F1AS4) that showed substantial biomass production in the presence of all three aromatic compounds were selected for further characterization of their oleaginous potential.

Lipid accumulation in aromatic compound-tolerant isolates

The evaluation of lipogenic capacity in phenol-free GMY medium after 120 h of cultivation revealed lipid contents ranging from 4.40% to 55.81% of cell dry weight (CDW) (Table 1). This notable metabolic variability was also reflected in biomass production, which reached a maximum of 13.35 g L^{-1} in isolate F6BS1.

Seven strains (F1AC4, F2AS1, F2AS3, F4AC1, F7BC1, F6BS1, and F1AS4) met the oleaginous threshold (> 20% lipid content), with F6BS1 and F2AS1 exhibiting the highest accumulation levels at 55.8% and 51.6%, respectively. Although bark-derived isolates frequently displayed high aromatic tolerance, the highest lipid accumulation was observed in soil-derived strains.

The isolate F6BS1 exhibited the highest volumetric lipid productivity (Q_L = 0.0621 g L^{-1} h^{-1}) and biomass productivity (Q_X = 0.1112 g L^{-1} h^{-1}), as well as the highest absolute lipid titer (7.45 g L^{-1}). Isolate F6BS1 also outperformed F2AS1, the second-best candidate, by 31% in Q_L and 21% in Q_X, while simultaneously achieving the highest biomass and lipid titers. Based on this performance profile, F6BS1 was selected for further characterization.

Table 1

Lipid production, volumetric productivity, and yields of yeast isolates tolerant to aromatic compounds. This table presents lipid production data for 13 yeast isolates capable of growing in the presence of aromatic compounds. Key metrics include biomass, lipid production, and glucose consumption (g L^{-1}), lipid accumulation (% w/w), volumetric productivities of lipids (Q_L) and biomass (Q_X) (g $L^{-1}h^{-1}$). Results are expressed as means ± standard deviation from three experiments. Values sharing the same letters are not significantly different (Tukey's test, α = 0.05)

Isolate	Biomass (g L^{-1})	Lipids (g L^{-1})	Glucose (g L^{-1})	Lipid (%)	Vol. Biomass $Q_{(x)}$	Vol. Lipids $Q_{(L)}$
F1AC2	7.95 ± 0.44^{c}	0.35 ± 0.03^{f}	24.79 ± 0.01^{gh}	4.40 ± 0.04^{i}	0.0663 ± 0.0002^{c}	0.0029 ± 0.0002^{f}
F1AC4	3.63 ± 0.23^{ef}	0.85 ± 0.03^{ef}	25.53 ± 0.33^{ef}	23.41 ± 0.01^{ef}	0.0302 ± 0.0009^{ef}	0.0071 ± 0.0012^{ef}
F2AS1	11.00 ± 0.05^{b}	5.68 ± 0.02^{b}	32.58 ± 0.06^{c}	51.63 ± 0.03^{ab}	0.0917 ± 0.0071^{b}	0.0473 ± 0.0038^{b}
F2AS3	3.65 ± 0.03^{ef}	1.28 ± 0.03^{de}	28.21 ± 0.02^{d}	34.90 ± 0.01^{cd}	0.0304 ± 0.0012^{ef}	0.0106 ± 0.0015^{de}
F4AC1	2.73 ± 0.02^{fg}	0.6 ± 0.03^{f}	26.02 ± 0.01^{e}	21.91 ± 0.01^{ef}	0.0227 ± 0.0015^{fg}	0.0050 ± 0.0012^{f}
F4AC2	2.88 ± 0.02^{fg}	0.54 ± 0.03^{f}	27.88 ± 0.01^{d}	18.87 ± 0.01^{efg}	0.024 ± 0.0032^{fg}	0.0045 ± 0.0002^{f}
F4AC3	3.33 ± 0.02^{ef}	0.5 ± 0.01^{f}	25.1 ± 0.07^{fg}	15.00 ± 0.03^{fgh}	0.0277 ± 0.0021^{ef}	0.0041 ± 0.0006^{f}
F4AC4	4.00 ± 0.01^{e}	0.45 ± 0.04^{f}	24.32 ± 0.01^{h}	11.30 ± 0.01^{ghi}	0.0333 ± 0.0012^{e}	0.0038 ± 0.0023^{f}
F7BC1	2.23 ± 0.03^{g}	0.75 ± 0.03^{ef}	10.3 ± 0.20^{k}	33.70 ± 0.01^{d}	0.0185 ± 0.0003^{g}	0.0063 ± 0.0010^{ef}
F7BC3	3.45 ± 0.02^{ef}	0.55 ± 0.01^{f}	12.78 ± 0.11^{j}	15.9 ± 0.01^{efgh}	0.0288 ± 0.0012^{ef}	0.0046 ± 0.0004^{f}
F6BS1	**13.35 ± 0.11^{a}**	**7.45 ± 0.15^{a}**	**37.14 ± 0.21^{a}**	**55.8 ± 0.01^{a}**	**0.1112 ± 0.0016^{a}**	**0.0621 ± 0.0006^{a}**
F6AC1	2.98 ± 0.02^{fg}	0.25 ± 0.03^{f}	21.46 ± 0.04^{i}	8.68 ± 0.02^{hi}	0.0244 ± 0.0021^{efg}	0.0021 ± 0.0006^{f}
F1AS4	11.03 ± 0.09^{b}	4.75 ± 0.03^{c}	35.12 ± 0.09^{b}	43.08 ± 0.03^{bc}	0.0919 ± 0.0001^{b}	0.0396 ± 0.0024^{c}

Growth kinetics and lipid production of selected F6BS1

Phenol exerted a concentration-dependent effect on the growth kinetics and lipid production of F6BS1. As shown in Fig. 1A, the maximum specific growth rate was comparable in the absence of phenol and at 0.5 g L^{-1}, whereas a marked reduction was observed at 1.0 g L^{-1}. Volumetric lipid productivity followed a similar pattern (Fig. 1B), with no significant difference between the control and the 0.5 g L^{-1} phenol treatment, while the highest phenol concentration substantially reduced productivity. Based on this inhibitory effect, the 1.0 g L^{-1} condition was excluded from subsequent kinetic analyses.

The time-course profiles under 0 and 0.5 g L^{-1} phenol further characterized the response of F6BS1 (Fig. 1C–F). Biomass accumulation (Fig. 1C) and lipid production (Fig. 1D) increased throughout cultivation under both conditions, although differences were observed during the initial stages. By the later sampling points, both treatments reached similar levels of biomass and lipid accumulation. Glucose consumption increased over time in both treatments (Fig. 1E), while the culture pH decreased from approximately 5.5 to around 4.5 (Fig. 1F). Overall, these results indicate that exposure to 0.5 g L^{-1} phenol did not prevent sustained biomass and lipid accumulation under the conditions tested.

Molecular identification of F6BS1

Molecular analyses placed isolate F6BS1 within the genus Solicoccozyma, clustering closely with S. phenolica based on the concatenated ITS and D1/D2 LSU rDNA sequences. Although minor sequence differences were observed, the available data do not by themselves establish that F6BS1 represents a distinct species. Further taxonomic assessment using additional loci and, where appropriate, complementary phenotypic or genomic evidence would be required to resolve its species-level status.

Microscopic characterization showed that cells grown in GMY medium for 120 h exhibited ovoid to ellipsoidal morphology and reproduced by budding. Fluorescence microscopy using Nile Red staining revealed the presence of intracellular lipid bodies, which were more abundant in cells exposed to 0.5 g L^{-1} phenol compared to the control. Calcofluor White staining showed uniform fluorescence consistent with intact cell walls and unicellular morphology (Fig. 2B).

Phenol degradation pathway in selected strain

Residual phenol levels decreased progressively during cultivation, reaching 0.088 ± 0.003 g L^{-1} at 120 h, corresponding to approximately 82% removal of the initial phenol content (Table 2). Catechol 1,2-dioxygenase activity increased over time, reaching 0.304 ± 0.039 U mg^{-1} at 120 h, whereas catechol 2,3-dioxygenase activity was not detected under the evaluated conditions. An inverse trend between residual phenol concentration and catechol 1,2-dioxygenase activity was observed throughout the cultivation period.

Table 2

Phenol removal and enzymatic activity over time in F6BS1. Phenol equivalents (g L^{-1}), total enzymatic activity (U), and specific enzymatic activity (U mg^{-1} protein) were determined at 24, 72, and 120 h in F6BS1 cultures. Results means ± standard deviation from three experiments

Time (h)	Residual phenol (g L^{-1})	Total enzymatic activity (U)	Specific enzymatic activity (U mg^{-1})
24	0.376 ± 0.041	0.027 ± 0.003	0.040 ± 0.003
72	0.168 ± 0.016	0.126 ± 0.021	0.166 ± 0.037
120	0.088 ± 0.003	0.218 ± 0.030	0.304 ± 0.039

Fatty acid methyl ester profile of selected strain

The fatty acid composition of F6BS1 was compared with that of vegetable oils and other oleaginous yeasts (Table 3). Across all conditions, F6BS1 exhibited a lipid profile dominated by C16:0 (25.60–27.06%) and C18:1 (51.56–54.06%). Although the 1 g L^{-1} phenol condition was excluded from kinetic analysis, its lipid profile was included to assess the effect of severe phenol stress on fatty acid composition. Minor variations were observed across all phenol concentrations, with no major shifts in the dominant fatty acids C16:0 and C18:1. The proportion of C18:1 in F6BS1 was higher than that reported for soybean oil (25.00%) and comparable to palm oil (46.10%). The content of C16:0 in F6BS1 was higher than that reported for soybean oil (10.90%) but lower than that of palm oil (36.17%). Linoleic acid (C18:2) content in F6BS1 ranged from 6.99 to 9.26%, which was lower than in soybean oil (52.70%) and similar to palm oil (8.60%).

When compared with other oleaginous yeasts, including *S. aeria*, *S. terricola*, and *R. glutinis*, F6BS1 showed a similar predominance of C16 and C18 fatty acids. However, differences were observed in the relative abundance of polyunsaturated fatty acids, particularly C18:2 and C18:3. Minor fatty acids, including C14:0, C15:0, C17:0, and C24:0, were present in low proportions (< 1%) across all F6BS1 conditions.

Table 3

Fatty Acid Methyl Ester (FAME) composition of F6BS1 oils compared to vegetable oils and other oleaginous yeasts. This table presents the composition of Fatty Acid Methyl Esters (FAME) in the oils of F6BS1 isolate, comparing them with vegetable oils and other oleaginous yeasts. The values indicate the relative abundance of fatty acids (w/w %) in each oil sample. ND denotes values that were not determined. This comparison highlights the fatty acid profiles of yeast oils compared to commonly used vegetable oils and other microbial sources of lipids

FAME	F6BS1			Soybean	Palm	*S. aeria*	*S. terricola*	*R. glutinis*
	0 g L^{-1}	0.5 g L^{-1}	1 g L^{-1}					
C14:0	0.28	0.26	0.22	0.10	0.70	ND	ND	1.29
C15:0	0.04	0.03	0.03	ND	ND	ND	ND	0.78
C16:0	27.06	26.88	25.60	10.90	36.17	20.67	26.17	16.78
C16:1	0.63	0.72	0.61	0.10	0.1	0.20	0.41	1.81
C17:0	0.67	0.64	0.54	ND	ND	0.08	ND	ND
C17:1	0.21	0.19	0.17	ND	ND	ND	ND	ND
C18:0	9.22	10.80	8.56	4.20	6.60	4.89	6.31	1.35
C18:1	51.56	52.36	54.06	25.00	46.10	63.81	63.12	61.60
C18:2	9.26	6.99	9.07	52.70	8.60	10.08	3.98	11.64
C18:3	ND	ND	ND	6.20	0.30	ND	ND	4.23
C20:0	0.43	0.54	0.44	ND	0.60	0.09	ND	ND
C22:0	0.09	0.13	0.10	ND	0.10	ND	ND	ND
C22:2	0.18	ND	0.28	ND	ND	ND	ND	ND
C24:0	0.37	0.46	0.32	ND	0.10	0.14	ND	ND
	This Study			(Ramos et al., 2009)		(Filippucci et al., 2016)		(Maza et al., 2020)

Biodiesel properties based on FAME's characterization

The quality of biodiesel is strongly influenced by the fatty acid composition of the feedstock, as well as production and post-processing conditions. In this study, the theoretical biodiesel properties of F6BS1 were evaluated based on its fatty acid profile, and the results are summarized in Table 4. These properties were analyzed at three phenol concentrations (0, 0.5, and 1 g L^{-1}) and compared with established standards, including ASTM D6751 (USA) and EN 14214 (Europe).

Regarding physicochemical properties, the predicted density (~ 0.86 g/cm³) and kinematic viscosity (4.53–4.57 mm^2 s^{-1}) fall within the limits specified by EN 14214, indicating suitable fuel flow behavior.

The iodine value (IV), reflecting the degree of unsaturation, ranged from 60.68 to 64.34 g I_2/100 g, remaining well below the maximum threshold (120 g I_2/100 g), while the cetane number (CN) ranged from 58.64 to 59.45, meeting international biodiesel standards. The estimated cold filter plugging point (CFPP) ranged from 8.88 to 14.12°C, reflecting the relatively high saturated fatty acid content and indicating limited low-temperature operability, which would restrict its use to warm climates or require blending or additives. Overall, most predicted properties fell within the ranges specified by ASTM D6751 and EN 14214; however, these are theoretical estimates derived from the fatty acid profile and do not substitute for experimental characterization of the fuel.

Table 4

Estimated biodiesel properties based on the fatty acid profile from F6BS1 isolate in comparison with international standards ASTM D6751 and EN 14214.
This table presents the theoretical biodiesel properties derived from the fatty acid profiles of F6BS1 isolate, compared with the specifications outlined in the international biodiesel standards ASTM D6751 and EN 14214. NS: Not specified by international biodiesel standard; SFA: Saturated Fatty Acids, MUFA: Monounsaturated Fatty Acids, PUFA: Polyunsaturated Fatty Acids, SV: Saponification Value, IV: Iodine Value, CN: Cetane number, OS: Oxidation Stability, DU: Degree of Unsaturation, LCSF: Long Chain Saturated Factor, CFPP: Cold Filter Plugging Point (°C), HHV: Higher Heating Value, υ: Kinematic Viscosity, ρ: Density

	F6BS1			**ASTM D6751**	**EN 14214**
	0 g L^{-1}	**0.5 g L^{-1}**	**1 g L^{-1}**		
SFA (wt %)	38.26	39.93	36.08	NS	NS
MUFA (wt %)	52.19	53.08	54.67	NS	NS
PUFA (wt %)	9.44	6.99	9.35	NS	NS
DU (wt %)	71.07	67.06	73.37	NS	NS
SV (mg KOH)	203.54	203.65	203.61	NS	NS
IV (gI_2/100g)	64.34	60.68	66.48	NS	<= 120
CN	58.64	59.45	58.15	>=47	>= 51
LCSF (wt %)	8.56	9.74	8.07	NS	NS
CFPP (°C)	10.42	14.12	8.88	NS	5 to 20
CP (°C)	9.24	9.15	8.47	NS	NS
OS (h)	15.33	19.46	15.59	NS	>= 6
HHV (MJ/Kg)	39.47	39.52	39.56	NS	~ 35
υ (mm^2 s^{-1})	4.53	4.57	4.53	1.96-6	3.5-5
ρ (g /cm^3)	0.86	0.87	0.87	NS	0.86–0.90

Discussion

Basidiomycetes predominated among bark-derived isolates, consistent with their well-established association with lignin-rich substrates and capacity to metabolize complex aromatic molecules (Yalçın et al., 2021). Ascomycetes, by contrast, were more frequently isolated from soil samples, where they typically dominate fungal communities and contribute to the degradation of plant-derived organic matter (Egidi et al., 2019; Manici et al., 2024). Genomic evidence further supports this ecological differentiation, indicating that Ascomycetes possess a higher number of genes encoding sugar transporters, which enhances their ability to utilize simple carbohydrates derived from decomposing substrates (de Vries, 2025).

Despite the initial diversity of isolates, all oleaginous strains belonged to Basidiomycota, in agreement with previous studies highlighting the metabolic versatility of this group for lipid accumulation and the utilization of complex substrates (Yaguchi et al., 2020). Forest ecosystems dominated by coniferous species such as *Podocarpus parlatorei*, characterized by high C/N litter and the accumulation of lignin-derived phenolic compounds, may act as ecological filters favoring microorganisms capable of both aromatic tolerance and efficient carbon storage (Jiang et al., 2025; Smolander and Kitunen, 2021).

The selection of F6BS1 was based on its superior volumetric productivities compared to other oleaginous candidates. Volumetric productivity was prioritized over lipid content alone, as it reflects process efficiency under time constraints relevant to industrial applications (Karamerou and Webb, 2019).

The growth inhibition of F6BS1 observed at phenol concentrations above 0.5 g L^{-1} is consistent with previous reports in basidiomycetous yeasts such as *Rhodotorula* species (Patel et al., 2017; Singh et al., 2022). However, higher tolerance levels have been reported in species such as *Candida tropicalis* SHC-03, which can grow at phenol concentrations exceeding 2 g L^{-1} (Li et al., 2024), highlighting the species-specific nature of phenol tolerance. The moderate resistance observed in F6BS1 suggests that process optimization strategies, such as increasing inoculum size, could further enhance its performance, as previously reported (Singh et al., 2022).

The increase in biomass during later cultivation stages may be associated with continued accumulation of storage compounds, particularly lipids (Lei et al., 2024). Notably, lipid production by F6BS1 at 0.5 g L^{-1} phenol (7.83 g L^{-1}) falls within or exceeds the range reported for other phenol-tolerant oleaginous yeasts, including *Rhodotorula kratochvilovae* HIMPA1, *Cryptococcus psychrotolerans*, and *Rhodotorula toruloides* (Deeba et al., 2018; Patel et al., 2017; Singh et al., 2022). The near-complete glucose consumption and the progressive decrease in pH further indicate active metabolism and the production of acidic by-products. The similarity of these profiles under control and phenol conditions suggests that, after adaptation, phenol does not impose a sustained metabolic burden. Moreover, the relative stability of pH during the stationary phase may indicate limited citrate accumulation, possibly due to its efficient channeling toward lipid biosynthesis or secretion dynamics (Karamerou and Webb, 2019).

Phylogenetic analysis placed F6BS1 close to *S. phenolica*, with minimal divergence in the ITS and D1/D2 regions. Because these markers have limited resolution among closely related *Solicoccozyma* species, (Liu et al., 2015; Scorzetti et al., 2002), F6BS1 is conservatively referred to as *Solicoccozyma* sp., multilocus analyses would be required to resolve its species-level identity. Although the genus *Solicoccozyma* remains relatively understudied, several species have demonstrated biotechnological potential, including glyphosate degradation by *Solicoccozyma terricola* (Stosiek et al., 2019) and indole-3-acetic acid production by *Solicoccozyma terrea* (Carvajal et al., 2024). Members of this genus are frequently isolated from montane forest soils and may exhibit psychrophilic traits (Sannino et al., 2017; Turchetti et al., 2025; Yurkov et al., 2025), supporting their potential for applications under diverse environmental conditions.

From a bioprocess perspective, the strictly unicellular morphology observed in F6BS1 is advantageous, as filamentous growth in yeasts is often associated with increased broth viscosity and limitations in mass transfer (El Enshasy, 2022). In contrast to observations in *Rhodotorula* species, where phenol exposure has been associated with increased lipid droplet size, F6BS1 did not exhibit noticeable changes in lipid droplet size under phenol exposure (Patel et al., 2017; Singh et al., 2024). This suggests that lipid accumulation may occur primarily through an increase in lipid droplet number rather than size, indicating a potentially distinct regulatory mechanism.

The enzymatic activity profile observed in F6BS1 is consistent with phenol degradation via the ortho-cleavage pathway, in which aromatic intermediates are metabolized through the β-ketoadipate route (Deeba et al., 2018). This pathway generates key intermediates such as acetyl-CoA and pyruvate, which serve as precursors for fatty acid biosynthesis and suggest a coupling between phenol removal and lipid accumulation (Yaguchi et al., 2020).

The fatty acid profile of F6BS1, dominated by C16 and C18 species, is characteristic of oleaginous yeasts (Fakas, 2017). The stability of the fatty acid profile across all phenol concentrations, including the inhibitory condition of 1 g L^{-1}, suggests that lipid quality is preserved even under severe aromatic stress. The minimal increase in C18:1 under phenol exposure may be associated with the activity of Δ-9 desaturase, which converts C18:0 to C18:1 as part of an adaptive response to environmental stress (Patel et al., 2017; Yaguchi et al., 2020). The presence of minor long-chain fatty acids further suggests an extended biosynthetic capacity, as reported in related yeasts (Filippucci et al., 2016).

From a fuel perspective, the relatively high proportion of monounsaturated fatty acids (MUFA), combined with moderate saturated fatty acids (SFA) and low polyunsaturated fatty acids (PUFA), is favorable for biodiesel quality (Knothe, 2006). The balance observed in F6BS1 supports desirable properties such as cetane number, viscosity, and oxidative stability. The iodine value remained well below the maximum threshold, while the cetane number met international standards, suggesting good ignition quality (de Jesus et al., 2020). The relatively high CFPP values (8.9–14.1°C), associated with the saturated fatty acid fraction, represent a limitation for use in cold climates, as also reported for other palmitic-rich microbial oils (Alptekin and Canakci, 2011; Wang et al., 2011). The estimated fuel-related properties derived from

the fatty acid profile suggest that F6BS1 lipids may have potential for biodiesel production. However, these estimates do not establish compliance with ASTM D6751 or EN 14214, which would require experimental characterization of the resulting biodiesel (Hazrat et al., 2021).

Taken together, these results position F6BS1 as a promising microbial platform for the valorization of phenol-rich waste streams, enabling the integration of aromatic compound degradation with lipid production. This dual functionality highlights its potential for sustainable bioprocesses coupling bioremediation with the generation of value-added products, such as those derived from agro-industrial residues including sugarcane vinasse and brewery wastewater (Ahmed et al., 2022; Pasquet et al., 2024).

Conclusion

This study highlights the potential of forest-derived oleaginous yeasts as promising resources for biotechnological applications involving aromatic pollutant removal and microbial lipid production. The characterization of *Solicoccozyma* sp. F6BS1 expands current knowledge of the metabolic versatility of this relatively understudied genus, demonstrating its capacity to sustain lipid accumulation under phenol exposure. The observed enzymatic activity further suggests the involvement of an ortho-cleavage pathway in phenol transformation, providing a basis for future metabolic investigations. Overall, these findings support the potential of *Solicoccozyma* as a microbial platform for integrating pollutant removal with the production of value-added lipids, although further validation in complex industrial effluents is required to establish its practical applicability.

Declarations

Competing Interests

The authors have no relevant financial or non-financial interests to disclose.

Funding Sources

This work was supported by the Agencia Nacional de Promoción de la Investigación, Desarrollo Tecnologico y la Innovación (ANPCyT) through PICT 2021-I A No. 0793; CONICET trough PIETR 298 202501 00114 CO and the Universidad Nacional de Tucuman through PIUNT G-739 and PIUNT D-742. 637

Author Contribution

F.G.D. and N.D.A.R. contributed equally to this work. F.G.D. and N.D.A.R. performed the experiments, analyzed the data, prepared the figures and tables, and wrote the original draft. M.S.P. performed the experiments and contributed to data analysis. C.G.N.P. and H.F.P. conceptualized the study, supervised

the research, and acquired funding. All authors reviewed and edited the manuscript and approved the final version.

Data Availability

The nucleotide sequence generated in this study is available in the NCBI GenBank database under accession number PQ757926. Additional data supporting the findings of this study are available from the corresponding author upon reasonable request.

References

1. Abeln F, Chuck CJ (2021) The history, state of the art and future prospects for oleaginous yeast research. Microb Cell Fact. https://doi.org/10.1186/s12934-021-01712-1
2. Ahmaruzzaman M, Mishra SR, Gadore V, Yadav G, Roy S, Bhattacharjee B, Bhuyan A, Hazarika B, Darabdhara J, Kumari K (2024) Phenolic compounds in water: From toxicity and source to sustainable solutions–An integrated review of removal methods, advanced technologies, cost analysis, and future prospects. J Environ Chem Eng 12:112964. https://doi.org/10.1016/j.jece.2024.112964
3. Ahmed PM, Nieto-Peñalver CG, de Figueroa LIC, Pajot HF (2022) Vinasse odyssey: sugarcane vinasse remediation and laccase production by Trametes sp. immobilized in polyurethane foam. Biodegradation 33:333–348. https://doi.org/10.1007/s10532-022-09985-y
4. Alptekin E, Canakci M (2011) Optimization of transesterification for methyl ester production from chicken fat. Fuel 90:2630–2638. https://doi.org/10.1016/j.fuel.2011.03.042
5. Altschul SF, Madden TL, Schäffer AA, Zhang J, Zhang Z, Miller W, Lipman DJ (1997) Gapped BLAST and PSI-BLAST: a new generation of protein database search programs. Nucleic Acids Research. Oxford University Press. https://doi.org/10.1093/nar/25.17.3389
6. Bligh EG, Dyer WJ (1959) A rapid method of total lipid extraction and purification. Can J Biochem Physiol 37:911–917
7. Buzzini P (2001) Batch and fed-batch carotenoid production by Rhodotorula glutinis–Debaryomyces castellii co-cultures in corn syrup. J Appl Microbiol 90:843–847. https://doi.org/10.1046/j.1365-2672.2001.01319.x
8. Carvajal M, Godoy L, Gebauer M, Catrileo D, Albornoz F (2024) Screening for indole-3-acetic acid synthesis and 1-aminocyclopropane-carboxylate deaminase activity in soil yeasts from Chile uncovers Solicoccozyma terrea as an effective plant growth promoter. Plant Soil 496:83–93. https://doi.org/10.1007/s11104-023-05906-x
9. de Jesus SS, Ferreira GF, Moreira LS, Filho RM (2020) Biodiesel production from microalgae by direct transesterification using green solvents. Renew Energy 160:1283–1294. https://doi.org/10.1016/j.renene.2020.07.056

10. de Vries RP (2025) Colony differentiation of saprobic and pathogenic fungi in relation to carbon utilization. Fungal Genet Biol 179:104001. https://doi.org/10.1016/j.fgb.2025.104001
11. Deeba F, Pruthi V, Negi YS (2018) Aromatic hydrocarbon biodegradation activates neutral lipid biosynthesis in oleaginous yeast. Bioresour Technol 255:273–280. https://doi.org/10.1016/J.BIORTECH.2018.01.096
12. Doyle J (1991) DNA protocols for plants. Molecular Techniques in Taxonomy. NATO ASI Series, vol 57. Springer, Berlin, Heidelberg. https://doi.org/10.1007/978-3-642-83962-7_18
13. Duan W, Meng F, Cui H, Lin Y, Wang G, Wu J (2018) Ecotoxicity of phenol and cresols to aquatic organisms: A review. Ecotoxicol Environ Saf. https://doi.org/10.1016/j.ecoenv.2018.03.089
14. Egidi E, Delgado-Baquerizo M, Plett JM, Wang J, Eldridge DJ, Bardgett RD, Maestre FT, Singh BK (2019) A few Ascomycota taxa dominate soil fungal communities worldwide. Nat Commun 10:2369. https://doi.org/10.1038/s41467-019-10373-z
15. El Enshasy HA (2022) Fungal morphology: a challenge in bioprocess engineering industries for product development. Curr Opin Chem Eng 35:100729. https://doi.org/10.1016/J.COCHE.2021.100729
16. Entrocassi GS, Gavilán RG, Sánchez-Mata D (2020) Subtropical mountain forests of las yungas: vegetation and bioclimate. Springer. https://doi.org/10.1007/978-3-030-25521-3
17. Fakas S (2017) Lipid biosynthesis in yeasts: A comparison of the lipid biosynthetic pathway between the model nonoleaginous yeast Saccharomyces cerevisiae and the model oleaginous yeast Yarrowia lipolytica. Eng Life Sci. https://doi.org/10.1002/elsc.201600040
18. Filippucci S, Tasselli G, Scardua A, Di Mauro S, Cramarossa MR, Perini D, Turchetti B, Onofri A, Forti L, Buzzini P (2016) Study of Holtermanniella wattica, Leucosporidium creatinivorum, Naganishia adeliensis, Solicoccozyma aeria, and Solicoccozyma terricola for their lipogenic aptitude from different carbon sources. Biotechnol Biofuels 9. https://doi.org/10.1186/s13068-016-0672-1
19. Guindon S, Dufayard JF, Lefort V, Anisimova M, Hordijk W, Gascuel O (2010) New algorithms and methods to estimate maximum-likelihood phylogenies: Assessing the performance of PhyML 3.0. Syst Biol 59:307–321. https://doi.org/10.1093/sysbio/syq010
20. Hall TA (1999) BioEdit: a user-friendly biological sequence alignment editor and analysis program for Windows 95/98/NT, in: Nucleic Acids Symposium Series. Oxford, pp. 95–98
21. Harzallah B, Grama SB, Bousseboua H, Jouanneau Y, Yang J, Li J (2023) Isolation and characterization of Indigenous Bacilli strains from an oil refinery wastewater with potential applications for phenol/cresol bioremediation. J Environ Manage 332:117322. https://doi.org/10.1016/J.JENVMAN.2023.117322
22. Hašek J (2006) Yeast Fluorescence Microscopy. In: Xiao W (ed) Yeast Protocol. Humana, Totowa, NJ, pp 85–96. https://doi.org/10.1385/1-59259-958-3:085
23. Hazrat MA, Rasul MG, Khan MMK, Mofijur M, Ahmed SF, Ong HC, Vo DVN, Show PL (2021) Techniques to improve the stability of biodiesel: a review. Environ Chem Lett. https://doi.org/10.1007/s10311-020-01166-8

24. Jiang Y, Lyu M, Lu Y, Deng C, Liu J, Wang M, Yang Y, Xie J (2025) Lignin–microbial necromass carbon coupling drives the vertical stratification mechanism of deep soil carbon sequestration in subtropical forests. J Appl Ecol 62:3550–3564. https://doi.org/10.1111/1365-2664.70215
25. Karamerou EE, Webb C (2019) Cultivation modes for microbial oil production using oleaginous yeasts – A review. Biochem Eng J 151:107322. https://doi.org/10.1016/J.BEJ.2019.107322
26. Kimura K, Yamaoka M, Kamisaka Y (2004) Rapid estimation of lipids in oleaginous fungi and yeasts using Nile red fluorescence. J Microbiol Methods 56:331–338. https://doi.org/10.1016/J.MIMET.2003.10.018
27. Knothe G (2006) Analyzing biodiesel: standards and other methods. J Am Oil Chem Soc 83:823–833. https://doi.org/10.1007/s11746-006-5033-y
28. Kruger NJ (2009) The Bradford Method For Protein Quantitation. In: Walker JM (ed) The Protein Protocols Handbook. Humana, Totowa, NJ, pp 17–24. https://doi.org/10.1007/978-1-59745-198-7_4
29. Kurtzman CP, Fell JW, Boekhout T The Yeasts - a Taxonomic Study. (5.), Elsevier BV (eds) (2011) https://shop.elsevier.com/books/the-yeasts/kurtzman/978-0-444-52149-1
30. Lei Y, Wang X, Sun S, He B, Sun W, Wang K, Chen Z, Guo Z, Li Z (2024) A review of lipid accumulation by oleaginous yeasts: Culture mode. Sci Total Environ 919:170385. https://doi.org/10.1016/J.SCITOTENV.2024.170385
31. Li Q, Chen Y, Tang H, Shu B, Zhang Z, Tang J, Li D, Jiang L, Shen J, Yang Y, Wang H, Ma M (2024) Unveiling superior phenol detoxification and degradation ability in Candida tropicalis SHC-03: a comparative study with Saccharomyces cerevisiae BY4742. Front. Microbiol. 15-2024.
32. Liu H, Yu QJ, Wang G, Ye F, Cong Y (2011) Biodegradation of phenol at high concentration by a novel yeast Trichosporon montevideense PHE1. Process Biochem 46:1678–1681. https://doi.org/10.1016/J.PROCBIO.2011.04.008
33. Liu J, Shen S, Zhu K, Li Z, Chen N, Lichtfouse E, Jia H (2024) Novel insights into the factors influencing rhizosphere reactive oxygen species production and their role in polycyclic aromatic hydrocarbons transformation. Soil Biol Biochem 198:109562. https://doi.org/10.1016/J.SOILBIO.2024.109562
34. Liu XZ, Wang QM, Göker M, Groenewald M, Kachalkin AV, Lumbsch HT, Millanes AM, Wedin M, Yurkov AM, Boekhout T, Bai FY (2015) Towards an integrated phylogenetic classification of the Tremellomycetes. Stud Mycol 81:85–147. https://doi.org/10.1016/j.simyco.2015.12.001
35. Manici LM, Caputo F, Fornasier F, Paletto A, Ceotto E, De Meo I (2024) Ascomycota and Basidiomycota fungal phyla as indicators of land use efficiency for soil organic carbon accrual with woody plantations. Ecol Indic 160:111796. https://doi.org/10.1016/j.ecolind.2024.111796
36. Maza DD, Viñarta SC, Su Y, Guillamón JM, Aybar MJ (2020) Growth and lipid production of Rhodotorula glutinis R4, in comparison to other oleaginous yeasts. J Biotechnol 310:21–31. https://doi.org/10.1016/J.JBIOTEC.2020.01.012
37. Miller GL (1959) Use of dinitrosalicylic acid reagent for determination of reducing sugar. Anal Chem 31:426–428

38. Minh BQ, Nguyen MAT, Von Haeseler A (2013) Ultrafast approximation for phylogenetic bootstrap. Mol Biol Evol 30:1188–1195. https://doi.org/10.1093/molbev/mst024
39. Nguyen LT, Schmidt HA, Von Haeseler A, Minh BQ (2015) IQ-TREE: A fast and effective stochastic algorithm for estimating maximum-likelihood phylogenies. Mol Biol Evol 32:268–274. https://doi.org/10.1093/molbev/msu300
40. O'Donnell K (1993) Fusarium and its near relatives. The Fungal Holomorph: Mitotic, Meiotic and Pleomorphic Speciation in Fungal Systematics/CBA International
41. Panigrahy N, Barik M, Sahoo RK, Sahoo NK (2020) Metabolic profile analysis and kinetics of p-cresol biodegradation by an indigenous Pseudomonas citronellolis NS1 isolated from coke oven wastewater. Int Biodeterior Biodegradation 147:104837. https://doi.org/10.1016/J.IBIOD.2019.104837
42. Pasquet PL, Bertagnolli C, Villain-Gambier M, Trébouet D (2024) Investigation of phenolic compounds recovery from brewery wastewater with coupled membrane and adsorption process. J Environ Chem Eng 12:112478. https://doi.org/10.1016/J.JECE.2024.112478
43. Patel A, Sartaj K, Arora N, Pruthi V, Pruthi PA (2017) Biodegradation of phenol via meta cleavage pathway triggers de novo TAG biosynthesis pathway in oleaginous yeast. J Hazard Mater 340:47–56. https://doi.org/10.1016/J.JHAZMAT.2017.07.013
44. Peralta MP, Aliaga J, Delgado OD, Fariña JI, Lechner BE (2021) *Paraboeremia yungensis* sp. nov., a new fungal species isolated from Las Yungas, South America, with promising tyrosinase production potential. Phytotaxa 528(3):191–201. https://doi.org/10.11646/phytotaxa.528.3.3
45. Pointing SB (1999) Qualitative methods for the determination of lignocellulolytic enzyme production by tropical fungi. Fungal Divers
46. Poontawee R, Lorliam W, Polburee P, Limtong S (2023) Oleaginous yeasts: Biodiversity and cultivation. Fungal Biol Rev 44:100295. https://doi.org/10.1016/J.FBR.2022.11.003
47. Ramalingam K, Venkatesan EP, Vellaiyan S, Mukhtar A, Sharifpur M, Yasir ASHM, Saleel CA (2023) Substitution of diesel fuel in conventional compression ignition engine with waste biomass-based fuel and its validation using artificial neural networks. Process Saf Environ Prot 177:1234–1248. https://doi.org/10.1016/j.psep.2023.07.085
48. Ramos MJ, Fernández CM, Casas A, Rodríguez L, Pérez Á (2009) Influence of fatty acid composition of raw materials on biodiesel properties. Bioresour Technol 100:261–268. https://doi.org/10.1016/J.BIORTECH.2008.06.039
49. Sánchez-Solís A, Lobato-Calleros O, Moreno-Terrazas R, Lappe-Oliveras P, Neri-Torres E (2024) Biodiesel Production Processes with Yeast: A Sustainable Approach. Energies (Basel). https://doi.org/10.3390/en17020302
50. Sannino C, Tasselli G, Filippucci S, Turchetti B, Buzzini P (2017) Yeasts in nonpolar cold habitats. Yeasts in Natural Ecosystems: Diversity. Springer, pp 367–396. https://doi.org/10.1007/978-3-319-62683-3_12

51. Sapsirisuk S, Polburee P, Lorliam W, Limtong S (2022) Discovery of Oleaginous Yeast from Mountain Forest Soil in Thailand. J Fungi 8. https://doi.org/10.3390/jof8101100
52. Scorzetti G, Fell JW, Fonseca A, Statzell-Tallman A (2002) Systematics of basidiomycetous yeasts: a comparison of large subunit D1/D2 and internal transcribed spacer rDNA regions. FEMS Yeast Res 2:495–517. https://doi.org/10.1111/j.1567-1364.2002.tb00117.x
53. Shetty GR, Shetty VK (2016) Pathway identification, enzyme activity and kinetic study for the biodegradation of phenol by Nocardia hydrocarbonoxydans NCIM 2386. Desalin Water Treat 57:8789–8801. https://doi.org/10.1080/19443994.2015.1030700
54. Singh S, Behera AR, Ghosh S, Daverey A, Dutta K (2024) Biodegradation of phenolic derivatives by Rhodosporidium toruloides: Effect on growth, cell morphology, lipid and biodiesel production. J Water Process Eng 59:104961. https://doi.org/10.1016/J.JWPE.2024.104961
55. Singh S, Bharadwaj T, Verma D, Dutta K (2022) Valorization of phenol contaminated wastewater for lipid production by *Rhodosporidium toruloides* 9564T. Chemosphere 308, 136269. https://doi.org/10.1016/J.CHEMOSPHERE.2022.136269
56. Smolander A, Kitunen V (2021) Soil organic matter properties and C and N cycling processes: Interactions in mixed-species stands of silver birch and conifers. Appl Soil Ecol 160:103841. https://doi.org/10.1016/j.apsoil.2020.103841
57. Stosiek N, Terebieniec A, Ząbek A, Młynarz P, Cieśliński H, Klimek-Ochab M (2019) N-phosphonomethylglycine utilization by the psychrotolerant yeast Solicoccozyma terricola M 3.1.4. Bioorg Chem 93:102866. https://doi.org/10.1016/J.BIOORG.2019.03.040
58. Summerbell RC (1985) The Staining of Filamentous Fungi with Diazonium Blue B. Mycologia 77:587–593. https://doi.org/10.1080/00275514.1985.12025144
59. Sun S, Wan X, Bian Y, Wang S, Zhang J, Wang W (2023) Biologically evolved dual-pathway catalytic pattern indicating an efficient bioremediation strategy for phenol removal. Chem Eng J 454:140195. https://doi.org/10.1016/J.CEJ.2022.140195
60. Szczepańska P, Hapeta P, Lazar Z (2022) Advances in production of high-value lipids by oleaginous yeasts. Crit Rev Biotechnol. https://doi.org/10.1080/07388551.2021.1922353
61. Torres IF, Bastida F, Hernández T, Bombach P, Richnow HH, García C (2014) The role of lignin and cellulose in the carbon-cycling of degraded soils under semiarid climate and their relation to microbial biomass. Soil Biol Biochem 75:152–160. https://doi.org/10.1016/J.SOILBIO.2014.04.007
62. Turchetti B, Sannino C, Mugnai G, Buzzini P (2025) Psychrophilic and psychrotolerant yeasts. Extremophilic Yeasts. Springer, pp 109–175. https://doi.org/10.1007/978-3-031-97453-3_3
63. Velez P, Tapia-Torres Y, García-Oliva F, Gasca-Pineda J (2021) Small-scale variation in a pristine montane cloud forest: Evidence on high soil fungal diversity and biogeochemical heterogeneity. PeerJ 9. https://doi.org/10.7717/peerj.11956
64. Wang W, Zhang Q, Sun X, Chen D, Insam H, Koide RT, Zhang S (2020) Effects of mixed-species litter on bacterial and fungal lignocellulose degradation functions during litter decomposition. Soil Biol Biochem 141:107690. https://doi.org/10.1016/J.SOILBIO.2019.107690

65. Wang Y, Ma S, Zhao M, Kuang L, Nie J, Riley WW (2011) Improving the cold flow properties of biodiesel from waste cooking oil by surfactants and detergent fractionation. Fuel 90:1036–1040. https://doi.org/10.1016/J.FUEL.2010.11.013
66. White TJ, Bruns T, Lee S, Taylor J (1990) Amplification and direct sequencing of fungal ribosomal RNA genes for phylogenetics. PCR protocols: guide methods Appl 18:315–322. https://doi.org/10.1016/b978-0-12-372180-8.50042-1
67. Wu D, Yin C, Fan Y, Chi H, Liu Z, Jin G (2023) Effect of forest planting patterns on the formation of soil organic carbon during litter lignocellulose degradation from a microbial perspective. Front Microbiol 14. https://doi.org/10.3389/fmicb.2023.1327481
68. Wu P, Zhang Z, Luo Y, Bai Y, Fan J (2022) Bioremediation of phenolic pollutants by algae - current status and challenges. Bioresour Technol 350:126930. https://doi.org/10.1016/J.BIORTECH.2022.126930
69. Yaguchi A, Franaszek N, O'Neill K, Lee S, Sitepu I, Boundy-Mills K, Blenner M (2020) Identification of oleaginous yeasts that metabolize aromatic compounds. J Ind Microbiol Biotechnol 47:801–813. https://doi.org/10.1007/s10295-020-02269-5
70. Yalçın HT, Fındık B, Terzi Y, Uyar E, Shatila F (2021) Isolation and molecular identification of industrially important enzyme producer yeasts from tree barks and fruits. Arch Microbiol 203:1079–1088. https://doi.org/10.1007/s00203-020-02104-6
71. Yurkov A, Turchetti B, Buzzini P (2025) Microbial life in extreme habitats. Extremophilic Yeasts. Springer, pp 3–29. https://doi.org/10.1007/978-3-031-97453-3_1
72. Zhang D, Gao F, Jakovlić I, Zou H, Zhang J, Li WX, Wang GT (2020) PhyloSuite: An integrated and scalable desktop platform for streamlined molecular sequence data management and evolutionary phylogenetics studies. Mol Ecol Resour 20:348–355. https://doi.org/10.1111/1755-0998.13096

Figures

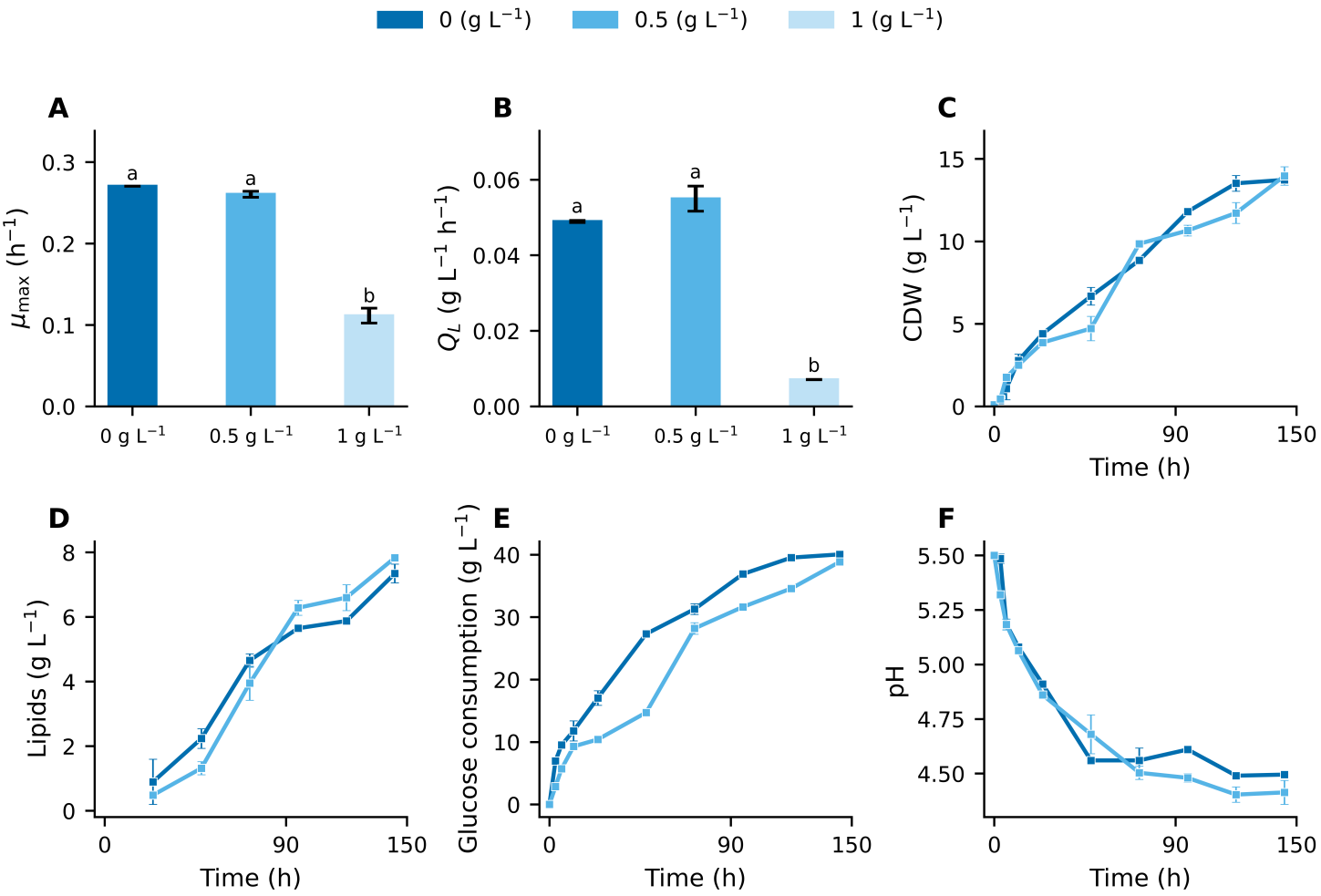


Figure 1

Effect of phenol concentration on growth kinetics and lipid production in Solicoccozyma sp. F6BS1. (A) Maximum specific growth rate (μmax) and (B) volumetric lipid productivity (Q_L) at increasing initial phenol concentrations (0, 0.5, and 1 g L^{-1}). (C–F) Time-course profiles in GMY medium supplemented with 0 or 0.5 g L^{-1} phenol: (C) cell dry weight, (D) lipid concentration, (E) glucose consumption, and (F) culture pH. Data are presented as mean ± standard deviation

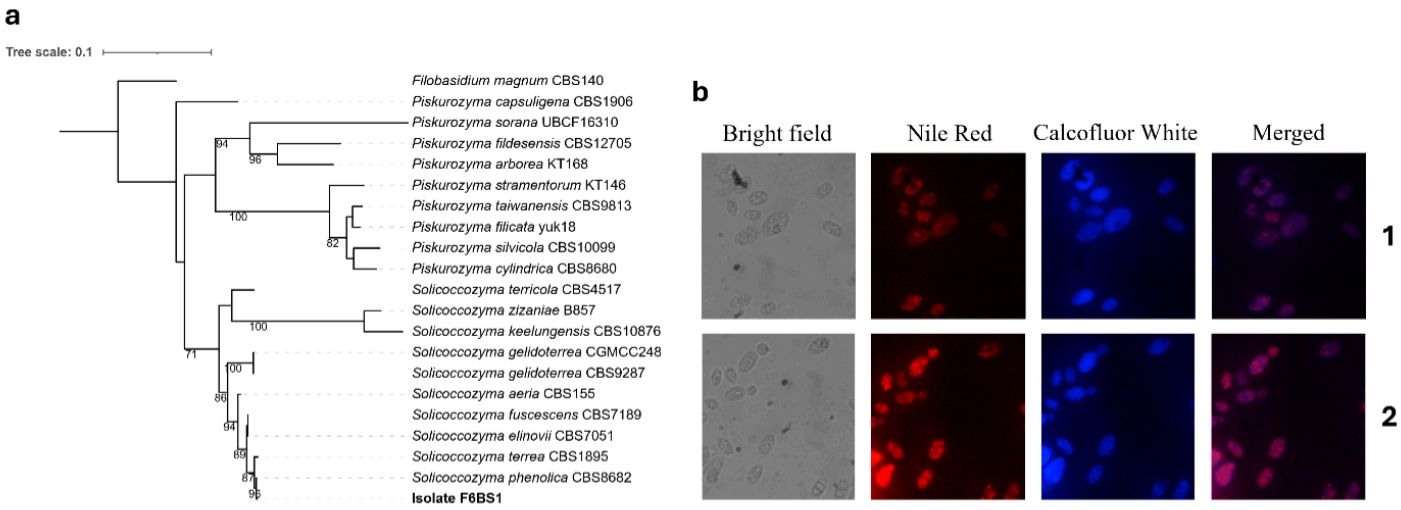


Figure 2

Phylogenetic placement and lipid accumulation of yeast isolate F6BS1 under phenol exposure. (a) Maximum Likelihood phylogenetic tree of the Piskurozymaceae family based on concatenated ITS and D1/D2 LSU rDNA sequences. Bootstrap values (>50%) are shown at branch nodes.
(b) Fluorescence microscopy of yeast cells grown in GMY medium for 120 h. Bright-field images (first column), lipid staining with Nile Red (red, second column), and cell wall staining with Calcofluor White (blue, third column); merged images are shown in the fourth column. Row 1: cells grown in the absence of phenol (0 g L^{-1}). Row 2: cells grown in the presence of phenol (0.5 g L^{-1}). Images were acquired at 100× magnification